ELSEVIER

Biochimica et Biophysica Acta 1508 (2000) 164–181

BIOCHIMICA ET BIOPHYSICA ACTA

BBA

www.elsevier.com/locate/bba

Review

Short-chain phospholipids as detergents

Helmut Hauser *

Institute of Biochemistry, Swiss Federal Institute of Technology, ETH Centre, Universitätsstrasse 16, CH-8092 Zurich, Switzerland

Received 19 April 2000; received in revised form 31 July 2000; accepted 1 August 2000

Abstract

The physico-chemical properties of short-chain phosphatidylcholine are reviewed to the extent that its biological activity as a mild detergent can be rationalized. Long-chain diacylphosphatidylcholines are typical membrane phospholipids that form preferentially smectic lamellar phases (bilayers) when dispersed in water. In contrast, the preferred phase of the short-chain analogues dispersed in excess water is the micellar phase. The preferred conformation and the dynamics of short-chain phosphatidylcholines in the monomeric and micellar state present in H_2O are discussed. The motionally averaged conformation of short-chain phosphatidylcholines is then compared to the single-crystal structures of membrane lipids. The main conclusion emerging is that in terms of preferred conformation and motional averaging short-chain phosphatidylcholines closely resemble their long-chain analogues. The dispersing power of short-chain phospholipids is emphasized in the second part of the review. Evidence is presented to show that this class of compounds is superior to most other detergents used in the solubilization of membrane proteins and the reconstitution of the solubilized proteins to artificial membrane systems (proteoliposomes). The prominent feature of the solubilization/reconstitution of integral membrane proteins by short-chain PC is the retention of the native protein structure and hence the protein function. Due to their special detergent-like properties, short-chain PC lend themselves very well not only to membrane solubilization but also to the purification of integral membrane proteins. The retention of the native protein structure in the solubilized state, i.e. in mixed micelles consisting of the integral membrane protein, intrinsic membrane lipids and short-chain PC, is rationalized. It is hypothesized that short-chain PC interacts primarily with the lipid bilayer of a membrane and very little if at all with the membrane proteins. In this way, the membrane protein remains associated with its preferred intrinsic membrane lipids and retains its native structure and its function.

Keywords: Short-chain detergent; Phosphatidylcholine; Membrane solubilization; Dispersing power; Integral membrane protein; Membrane reconstitution; Proteoliposome

Abbreviations: ap, antiperiplanar; BBM, brush border membrane(s); BBMV, brush border membrane vesicle(s); $C_{12}E_8$, poly(oxyethylene)-8-lauryl ether; cmc, critical micellar concentration(s); CTAB, cetyltrimethylammonium bromide; diC_6PC, 1,2-dihexanoyl-*sn*-glycero-3-phosphocholine; diC_7PC, 1,2-diheptanoyl-*sn*-glycero-3-phosphocholine; diC_8PC, 1,2-dioctanoyl-*sn*-glycero-3-phosphocholine; diC_9PC, 1,2-dinonanoyl-*sn*-glycero-3-phosphocholine; $diC_{14}PC$, 1,2-dimyristoyl-*sn*-glycero-3-phosphocholine; $diC_{16}PC$, 1,2-dipalmitoyl-*sn*-glycero-3-phosphocholine; DLPA, sodium-2,3-dilauroyl-D-glycero-1-phosphate monohydrate; $DLPEM_2$, 2,3-dilauroyl-DL-glycero-1-phospho-*N*,*N*-dimethylethanolamine; DMPCA, 2,3-dimyristoyl-D-glycero-1-phosphocholine dihydrate (the letter A at the end refers to conformation A, i.e. one of the two conformationally unique molecules of the crystal structure); DMPGA, sodium-2,3-dimyristoyl-D-glycero-1-phospho-DL-glycerol (for letter A see DMPCA); DSC, differential scanning calorimetry; DTAPS, 3-(dimethyltetradecylammonio)propane-1-sulfonate; NADH, reduced form of nicotinamide adenine dinucleotide; $NaDodSO_4$, sodium dodecyl sulfate; PC, phosphatidylcholine(s); PS, phosphatidylserine(s); sc, synclinal; SUV, small unilamellar vesicle(s)

* Corresponding author. Fax: +41 (1) 6321298; E-mail: helmut.hauser@bc.biol.ethz.ch

0005-2736/00/$ – see front matter
PII: S0304-4157(00)00008-3

1. Introduction

Short-chain phosphatidylcholines (PC) are structurally phospholipids, but their short fatty acyl chains of 6–8 C-atoms endow the molecule with detergent-like properties. These compounds form micelles rather than bilayers when dispersed in water with a relatively high critical micellar concentration (cmc) [1]. Good use has been made of the dispersing power and detergent properties of short-chain PC. They have been applied successfully in the solubilization of biological membranes and the reconstitution of membrane proteins into simple, well-defined membrane systems (proteoliposomes). One problem encountered in the solubilization/reconstitution of membrane proteins in the presence of detergents is the denaturation of the protein and the accompanying loss of enzymatic activity. Most detergents used in biology induce protein denaturation to some extent or at least in excess concentrations used in membrane solubilization/reconstitution procedures. Evidence is reviewed here showing that short-chain PC are mild detergents: they solubilize membrane proteins effectively, yet the native protein conformation and in turn the enzymatic activity are retained in the solubilized state over a rather large PC concentration range. In this respect short-chain PC are superior to most detergents that have been used so far in the solubilization/reconstitution of membrane proteins. Due to the special, detergent-like properties of short-chain phospholipids, this class of compounds has been successfully applied to the purification and crystallization of integral membrane proteins. The prospect of growing single crystals of integral membrane proteins suitable for single-crystal structure analysis is particularly attractive in the light that the three-dimensional structure of most integral membrane proteins is still elusive.

2. Critical micellar concentration (cmc)

Short-chain phospholipids differ from their long-chain counter part in terms of phase behavior. Short-chain phospholipids aggregate in aqueous solvents forming micelles rather than bilayers which are the preferred form of aggregation of long-chain membrane phospholipids. The values for the cmc of short-chain phosphatidylcholines decrease with increasing length of the hydrocarbon chains (Table 1) [1]. The cmc values of diC_6PC range from 11 to 16 mM depending on the method of determination used (average: 13.7 ± 1.6 mM or 6.5 ± 0.8 mg/ml) [1–7]. Applying the mass action law to the monomer-micelle association in the homologous series of diC_6PC, diC_7PC, diC_8PC and diC_9PC, the standard free energy of micellization ΔG^0 is given by

$$\Delta G^0 = -RT \ln K = -\frac{RT}{n} \ln[M_n] + RT \ln[M_1] \quad (1)$$

Table 1
Critical micellar concentrations of short-chain PC

Critical micellar concentration								Experimental conditions	Method	Ref.
$diC_6PC{\bullet}H_2O$		$diC_7PC{\bullet}H_2O$		$diC_8PC{\bullet}H_2O$		$diC_9PC{\bullet}H_2O$				
mg/ml	mM	mg/ml	mM	mg/ml	mM	mg/ml	μM			
6.9	14.6	0.71	1.42	0.14	0.27	0.016	28.8	10^{-2} M phosphate buffer pH 6.9	surface tension measurements	[1]
6.5	13.8	0.80	1.60	0.13	0.25	–	–	10^{-2} M phosphate buffer pH 6.9	light scattering	[1]
6.5	13.8	0.90	1.8	0.10	0.19	–	–	0.5 mM Tris pH 6.5, 0.1 M NaCl, 10 mM $CaCl_2$	surface tension measurements, and light scattering	[2]
7.54	16 ± 2	–	–	–	–	–	–	H_2O	calorimetry	[3]
7.2	15.2	–	–	–	–	–	–	^2H_2O pH ≈ 6	ultrafiltration	[4]
5.2	11.0	–	–	–	–	–	–	0.5 mM Tris pH 8, 0.01 M NaCl, 0.02 M $CaCl_2$, 0.7 mM EDTA	refractive index measurements	[5]
–	–	0.90	1.8	–	–	–	–	0.1 M NaCl pH 7.0	change in absorbance at 542 nm of rhodamine 6G in the presence of increasing concentrations of diC_7PC	[6]
7.2	15.2	–	–	–	–	–	–	H_2O	small-angle neutron scattering	[7]

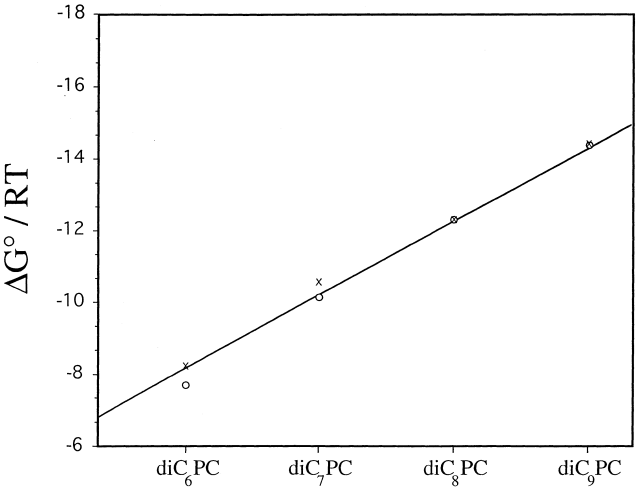

Fig. 1. Standard free energy ΔG^0 of micellization (at room temperature) for four short-chain PC. The values of ΔG^0 (×) were calculated from experimentally determined cmc values using Eq. 2, or alternatively Eq. 1 (open circles) (adapted from [1]).

where $[M_1]$ and $[M_n]$ are the concentrations of monomers and micelles, respectively, K is the association constant, n is the number of molecules per micelle, T is the absolute temperature and R the gas constant [1]. For large n values Eq. 1 reduces to

$$\Delta G^0 = RT \ln[M_1] = RT \ln[\text{cmc}] \quad (2)$$

The standard free energy of micellization ΔG^0 (in units of RT) is calculated for the homologous series of short-chain PCs using Eq. 1 [1]. Plotting these ΔG^0 values as a function of the hydrocarbon chain length yields a straight line (Fig. 1) from the slope of which a value for the standard free energy of micellization per mole of CH_2 group is derived: $\Delta G^0 = -0.88$ RT/mole of CH_2 group (2.1 kJ or 0.51 kcal/mole of CH_2 group). This value is in good agreement with ΔG^0 values reported for other surfactants ([1] and Refs. cited therein). Extrapolating the straight line in Fig. 1 to 16 C-atoms, i.e. to $diC_{16}PC$, yields a ΔG^0 value of -24.4 RT corresponding to a cmc of 2.5×10^{-11} M. This value may be compared to the experimental value of the cmc of $diC_{16}PC$ determined at room temperature by Smith and Tanford [8]. The experimental value of 4.6×10^{-10} M is about one order of magnitude higher than the value derived by extrapolation of the straight line in Fig. 1.

Concentrations of NaCl and other salts of up to several molar have the effect of reducing the cmc of short-chain PC. This phenomenon is interpreted as salting out of nonpolar solutes [1,9].

3. Micellar properties of short-chain phosphatidylcholines

Information on the aggregation number n and micellar weights of short-chain PC were derived from light scattering and ultracentrifugation using the sedimentation equilibrium method [9]. DiC_6PC appears to aggregate to micelles of an average weight of 15 000–20 000 with a narrow size distribution or low polydispersity. In contrast, both the micellar weight and the polydispersity of diC_7PC and diC_8PC micelles increase dramatically [9,10]. The micellar weight of diC_7PC micelles ranges from 20 000 to 100 000 depending on concentration. NaCl up to 3 M has little effect on the micellar weight of diC_7PC [9]. With diC_8PC dispersions the minimum micellar weight is 250 000 (aggregation number $n > 470$), and the micellar weight increases very strongly with concentration. Light scattering of diC_8PC dispersions is consistent with very large, extended structures [10].

Lin et al. [7] used small-angle neutron scattering to determine the size and shape of diC_6PC micelles. These micelles are described as monodisperse characterized by an aggregation number of $n = 19 \pm 1$ over the total concentration range of 0.027–0.361 M studied. The small-angle neutron scattering data of diC_6PC micelles are consistent with the shape of a prolate ellipsoid consisting of two uniform regions (Fig. 2). The inner region of the ellipsoid contains

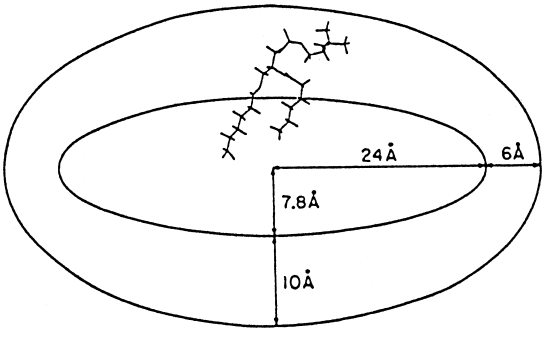

Fig. 2. Schematic drawing showing the shape of diC_6PC micelles as derived from small-angle neutron scattering of diC_6PC dispersions in water. The diC_6PC molecule inserted in the micelle is a PC molecule taken from the crystal structure of $diC_{14}PC$ with truncated hydrocarbon chains. From [7].

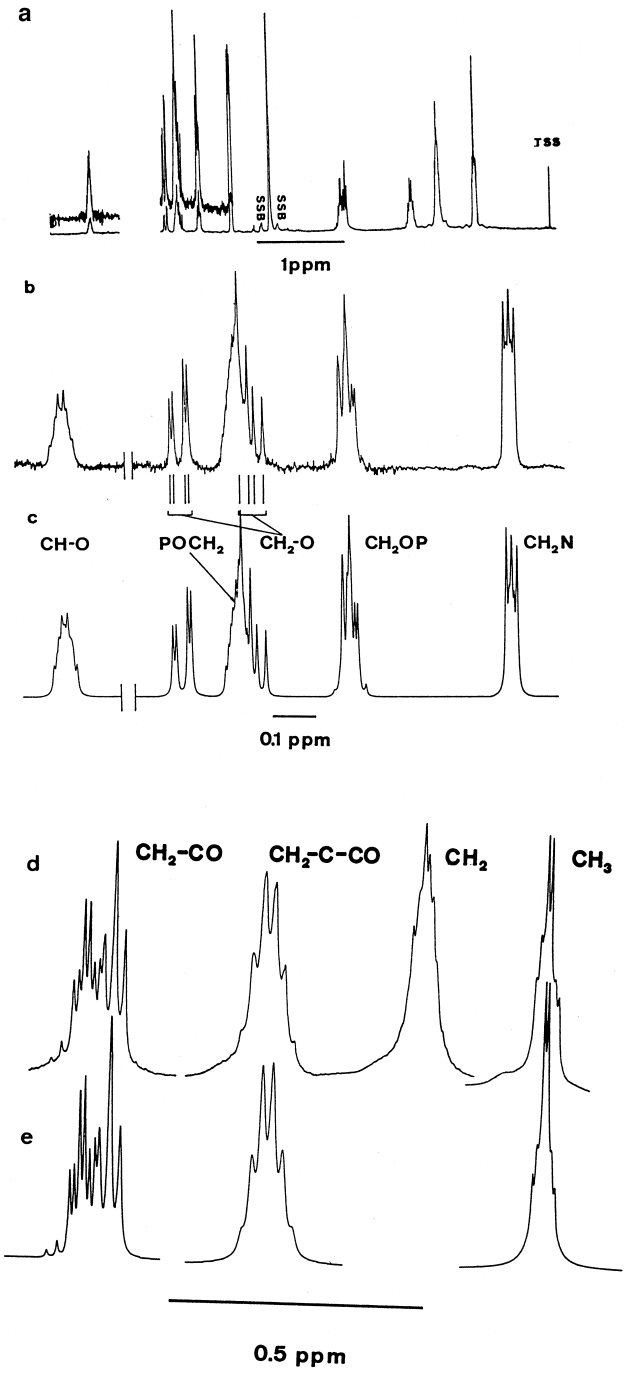

Fig. 3. 360 MHz ^{1}H-NMR spectrum of diC_6PC in ^2H_2O (approx. 10 mg lipid/ml = 21.2 mM) at a nominal pH of 6 recorded at 25°C (a). The expanded spectrum of the lipid polar group except for the $N(CH_3)_3$ resonance and the computer simulation of this spectrum are shown in b and c, respectively. In b and c the resonance of the single glycerol proton (C(2)H) is not at its correct chemical shift. SSB, spinning side band (from [4]). Signals of the hydrocarbon chains (d) and their computer simulations (e). The position of the hydrocarbon chain signals on the x-axis is arbitrary (from [19]).

the hydrocarbon chains, the outer region the PC polar head groups. The hydrocarbon chains form a close-packed core of spheroidal shape with a minor axis of 0.78 nm corresponding to fully extended hydrocarbon chains and a major axis of 2.4 nm. This hydrophobic core is surrounded by a shell of polar groups of thickness of 1 nm along the minor axis and 0.6 nm along the major axis (Fig. 2). In this shell region 80% of the volume is occupied by water and 20% by the polar head groups. The area per PC head group in the micellar structure is 1.02 nm^2 which considerably exceeds the area per head group (approx. 0.65 nm^2) in a PC monolayer or bilayer. This may at least partially be responsible for the observation that short-chain PC micelles are much better substrates for phospholipases than PC bilayers. Ap-

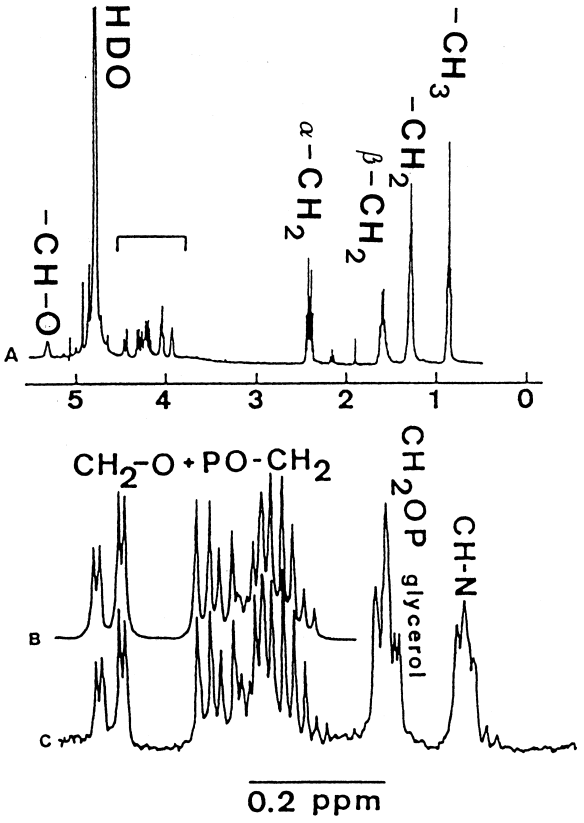

Fig. 4. 360 MHz ^{1}H-NMR spectrum of the NH_4^+ salt of diC_6PS in ^2H_2O (approx. 2 mg/ml = 4.2 mM) at a nominal pH of about 6 at 25°C. The overall spectrum with the assignment of resonances relative to sodium 3-(trimethylsilyl)propanesulfonate is shown in A. The expanded spectrum of the polar group region (see bracket in spectrum A) and the computer simulation of the CH_2-OCO signal and the PO-CH_2 serine signal are shown in C and B, respectively (from [20]).

Table 2
^{1}H-NMR chemical shifts of diC_6PC

Resonance	Chemical shifts (ppm)[a]		
	diC_6PC in ^2H_2O below the cmc (6.4 mM)	diC_6PC in ^2H_2O above the cmc (96 mM)	diC_6PC in $C^2H_3O^2H$
Terminal CH_3	0.87	0.883; 0.890[b]	0.912; 0.915[b]
$(CH_2)_n$	1.30	1.33	1.33
CH_2-C-CO	1.61	1.63	1.61
CH_2-CO	2.40; 2.42	2.36; 2.40; 2.43[c]	2.32; 2.34
CH_2-O-CO[d]	H_A = 4.28	4.29	4.17
	H_B = 4.43	4.47	4.42
CH-O-CO[d]	H_C = 5.32	5.34	5.23
CH_2-O-P[d]	H_D = 4.05	4.07	4.00
	H_E = 4.06	4.08	4.01
OP-CH_2	4.30	4.33	4.28
CH_2-N	3.66	3.71	3.64
$N(CH_3)_3$	3.22	3.27	3.22

[a]Chemical shifts are expressed in ppm downfield from sodium 3-(trimethylsilyl)propanesulfonate and tetramethylsilane used as internal references in ^2H_2O and organic solvents, respectively. The accuracy of the chemical shifts is ±0.005 ppm for the hydrocarbon resonances and 0.01 ppm for the polar group resonances [4].
[b]Chemical shifts of the two partially overlapping triplets.
[c]The α-methylene protons of diC_6PC in ^2H_2O above the cmc give rise to a complex multiplet consisting of a triplet at 2.36 ppm assigned to the α-methylene protons of the γ-chain and the AB part of an ABX_2 system assigned to the α-methylene protons of the β-chain. The AB protons resonate at 2.40 and 2.43 ppm.
[d]The lettering of the glycerol protons is as follows:

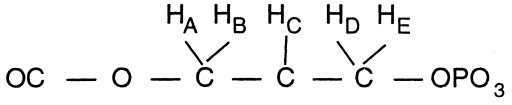

parently in these PC micelles with significantly larger interfacial areas per molecule, the PC head group is much better accessible to the phospholipase than in bilayers. Since the fully extended length of the PC polar group including the glycerol and the fatty acyl carbonyls exceeds 1 nm [11,12] and the thickness of the shell is 1 nm or smaller, the orientation of the phosphocholine group in diC_6PC micelles is very likely parallel to the micellar surface (cf. scheme in Fig. 2). This orientation is similar to that observed in PC bilayers [11–16].

4. Structure and dynamics of short-chain phospholipids

The conformational and motional properties of short-chain PC have been studied by high-resolution NMR. As discussed above unlike long-chain PC short-chain PC form small micelles. The overall tumbling of such small micelles and the molecular motions of individual lipid molecules within the micelle are sufficiently fast to average out dipolar broadening. As a result highly resolved NMR spectra are obtained. As examples the ^{1}H-NMR spectra of diC_6PC and diC_6PS are shown in Figs. 3 and 4, respectively. Well resolved high-resolution spectra

Table 3
Shift difference between α-methylene groups in the 220 MHz ^{1}H-NMR spectra of phosphatidylcholines in different mixed micellar systems (adapted from [18])

Detergent/phospholipid	Chemical shifts (ppm)		
	C(22) H_2 or *sn*-2 α-CH_2		C(32) H_2 or *sn*-1 α-CH_2
	H_A	H_B	
Triton X-100/diC_{16}PC	2.35		2.26
Triton X-100/diC_6PC	2.40	2.36	2.30
Triton X-100/diC_8PC	2.39	2.34	2.26
DTAPS/diC_{16}PC	2.43	2.35	2.30
CTAB/diC_{16}PC	2.43	2.33	2.28
$NaDodSO_4$/diC_{16}PC	2.40		2.32

with clearly discernible spin-spin coupling are obtained from short-chain phospholipids both below and above the cmc. Good use has been made of these compounds to study the effect of aggregation and solvation on the conformational properties of short-chain PC. Conformational information has been derived from vicinal homonuclear and heteronuclear spin-spin coupling constants as described in [4,17–22][1].

4.1. Inequality of the two hydrocarbon chains

With aqueous solutions of diC_6PC significant spectral changes are observed in both the hydrocarbon chain and the polar group signals of the ^{1}H-NMR spectra in the concentration range of the cmc [4,17]. The aggregation of diC_6PC to micelles is accompanied by a small but significant downfield shift of most of the hydrocarbon and polar group resonances (Table 2). The line width of all resonances increases in the concentration range of the cmc.

Roberts et al. [18] were the first to report on the chemical and magnetic inequality of the two hydrocarbon chains of short-chain PC. Short-chain and long-chain PC behaved similarly when incorporated in mixed detergent micelles as evident from ^{1}H-NMR (Table 3) [18]. In mixed micelles the α-methylene groups of short-chain PC give rise to a complex ^{1}H-NMR spectrum (Fig. 6) which apart from the line width is similar to that obtained from an aqueous diC_6PC dispersion above the cmc (cf. Figs. 3d and 6C) [18,19]. Decoupling of the β-methylene protons ($C(23)H_2$ and $C(33)H_2$) reduces the complex pattern to a single line and a partial quartet of an AB pattern downfield of the single line (Fig. 6D). This indicates that the protons of one of the two α-methylene groups are magnetically nonequivalent (cf. Table 3). The α-methylene group giving rise to the AB pattern at 2.33–2.43 ppm (Table 3) was identified as the $C(22)H_2$ group (*sn*-2 α-methylene) while the upfield resonance at 2.26–2.32 ppm (cf. Table 3) was assigned to the $C(32)H_2$ group (*sn*-1 α-methylene) [18].

Hauser et al. confirmed this assignment of the two α-methylene groups in the ^{1}H-NMR spectra of diC_6PC micelles. Based on shift and coupling constant data of ^{1}H-NMR [4,19] and ^{13}C-NMR [24] measurements it was concluded that the two hydrocarbon chains of short-chain PC micelles are chemically and magnetically nonequivalent.

The assignment of the two α-methylene groups is consistent with ^{13}C-NMR measurements carried out with aqueous dispersions of $diC_{16}PC$ and micellar dispersions of diC_6PC [23]. Both PC were synthesized with ^{13}C-enriched CO groups. An expanded ^{13}C-NMR spectrum of the CO region of $diC_{16}PC$ SUV is shown in Fig. 7. The low-field and the high-field peaks in spectrum A obtained from SUV of $diC_{16}PC$ ^{13}C-labeled in the C(21)-O group (*sn*-2 chain) are assigned to PC molecules in the outer and inner leaflet of the bilayer, respectively. SUV of $diC_{16}PC$ labeled in both carbonyl groups give rise to the ^{13}C-NMR spectrum B in which both low-field and high-field resonances are split. By comparison of spectra A and B (Fig. 7) the carbonyl group of the *sn*-1 chain can be assigned to the peaks about 0.1 ppm upfield to the signals arising from the *sn*-2 carbonyl group [23]. The same authors [23] showed that in micelles of diC_6PC the ^{13}C-NMR signal of the C(21)-O group (*sn*-2 chain) is downfield relative to that of the C(31)-O group (*sn*-1 chain). From a comparison of the ^{13}C-NMR spin-lattice relaxation times of short-chain PC

[1] Nomenclature. In discussing conformational and motional properties of short-chain phospholipids the structural notation presented in Fig. 5 is used (for a more detailed discussion see [11] and [12]). The glycerol C-atoms are regarded as the central part (backbone) of the molecule to which the α-, β- and γ-chains are linked. The β- and γ-chains are the hydrocarbon chains attached to glycerol C-atoms C(2) and C(3), respectively. The α-chain is the polar head group linked to glycerol atom C(1). In the atom numbering given in Fig. 5a, the first numeral (1, 2 or 3) refers to the α-, β- and γ-chain, respectively, while the second numeral represents the atom numbering which increases going from the glycerol group towards the end of the respective chain. For instance, the two α-methylene carbon atoms are C(22) for the β-chain and C(32) for the γ-chain. In the stereospecific numbering (*sn*-nomenclature) these two C-atoms are referred to as *sn*-2 α-methylene carbon and *sn*-1 α-methylene carbon, respectively. Using the atom numbering of Fig. 5a diC_6PC is designated as 2,3-dihexanoyl-D-glycero-1-phosphocholine, or alternatively, in the *sn*-nomenclature as 1,2-dihexanoyl-*sn*-3-phosphatidylcholine. Similarly, the NH_4^+ salt of diC_6PS is either NH_4-2,3-dihexanoyl-D-glycero-1-phospho-L-serine or NH_4-1,2-dihexanoyl-*sn*-3-phosphatidylserine. For the definition of the stereochemistry and the chirality of the C2-glycerol atom of phospholipids see [11,12]. The definition of torsion angles, the steric relationship of substituents of a single C-C bond and the notation of torsion angle ranges are given in panels b and c of Fig. 5.

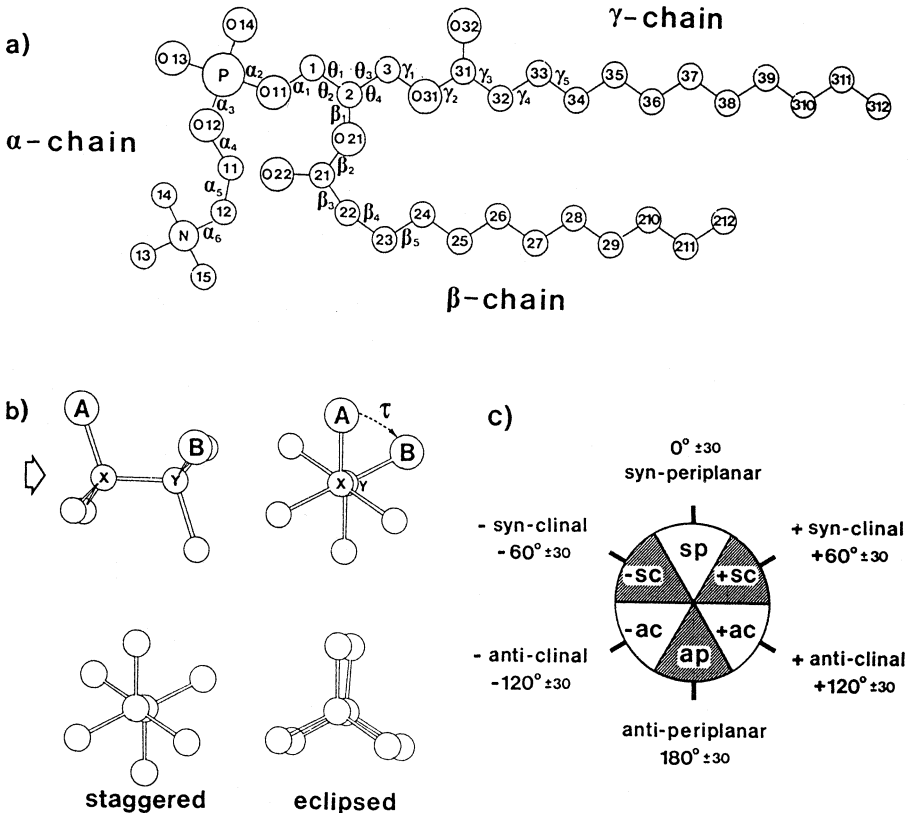

Fig. 5. Nomenclature used for conformational analyses of phospholipids. (a) Atom numbering and notation of torsion angles according to Sundaralingam [28]. (b) Definition of torsion angles. (c) Notation of torsion angle ranges according to Klyne and Prelog [29].

present in micelles with ^{2}H-NMR spin-lattice relaxation times of diC_{16}PC in bilayers [25], Burns et al. [24] proposed that similar relaxation mechanisms are at play in micelles and bilayers.

4.2. *Parallel alignment of the two hydrocarbon chains. Preferred conformation of the diacylglycerol part of short-chain phospholipids*

These results taken together are interpreted to mean that short-chain PC adopt a unique conformation in micellar dispersion, be it pure short-chain phospholipid micelles or mixed micelles with nonionic or ionic detergents. The resonances of the *sn*-1 α-methylene protons and *sn*-1 ^{13}CO group are upfield relative to the corresponding resonances of the *sn*-2 chain. This chemical shift difference and the nonequivalence of the *sn*-2 α-methylene protons indicate that the conformation of the initial segments of the β-chain (*sn*-2 chain) and γ-chain (*sn*-1 chain) are significantly different: the γ-chain (*sn*-1 chain)

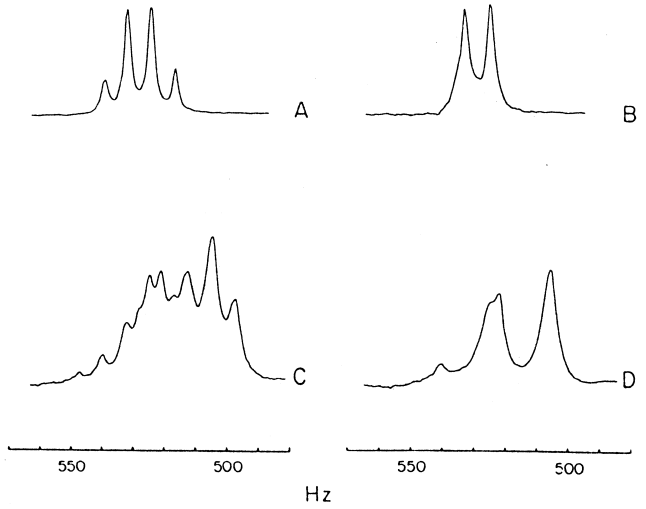

Fig. 6. ^{1}H-NMR spectra of the α-methylene protons (C(22)H_2 and C(32)H_2) of diC_6PC monomers without (A) and with decoupling of the adjacent CH_2 protons (β-methylenes) (B), and the α-methylene protons of diC_6PC in mixed Triton X-100/diC_6PC micelles of molar ratio 4:1 without (C) and with decoupling of the adjacent CH_2 groups (β-methylenes) (D). From [18].

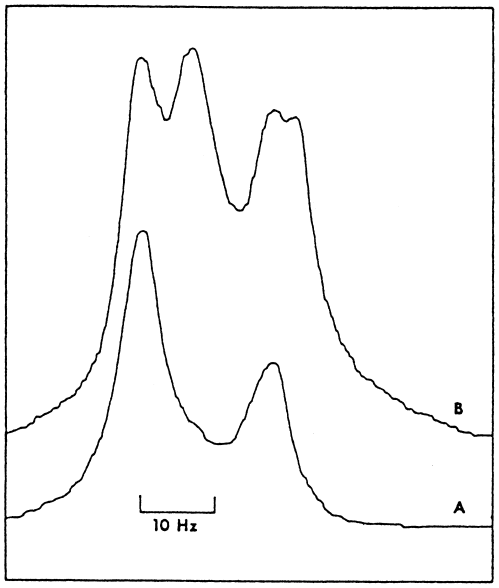

Fig. 7. ^{13}C-NMR spectra of SUV made of diC_{16}PC with a ^{13}C-labeled C(21)-O group (*sn*-2 chain) (A) and SUV made of diC_{16}PC with both CO groups being ^{13}C-labeled (B). SUV were made by tip sonication of the diC_{16}PC dispersion in 50 mM KCl at 45°C as described in [23].

appears to be in a more hydrophobic (shielded) environment than the corresponding segment of the β-chain (*sn*-2 chain). We note that the pronounced difference in conformation and chemical environment of the two hydrocarbon chains is a property of the aggregated (micellar) state. The structural and motional data discussed so far are consistent with the notion that short-chain phospholipids have a preferred conformation when aggregated in micelles and this preferred conformation closely resembles that of long-chain phospholipids present in mixed micelles (cf. Table 3).

More information concerning the conformational preference and motional averaging of short-chain phospholipids in both monomeric and micellar state has been derived from high-resolution NMR studies. The same vicinal spin-spin coupling constant analysis used to derive conformational and motional information of the two hydrocarbon chains has been applied to the lipid polar group [20].

The approximately parallel arrangement of the two hydrocarbon chains represents a fundamental packing mode of long-chain lipids encountered in most lipid aggregates (phases), particularly micelles and bilayers. The questions that arise in the discussion of the preferred conformation of short-chain phospholipids are whether or not the parallel chain stacking is maintained with the preferred conformation of this class of diacyl phospholipids, particularly in the monomeric state, and how this chain stacking is affected by different solvents. From ^{1}H-NMR of short-chain phospholipids dissolved or dispersed in different solvents, both below and above the cmc, it has been concluded that there is a preferred conformation about the C(2)-C(3) glycerol bond (Table 4). The three staggered conformations of minimum free energy about the glycerol C(2)-C(3) bond are shown in Fig. 8. These conformations are characterized by two related torsion angles θ_3 = C(1)-C(2)-C(3)-O(31) and θ_4 = O(21)-C(2)-C(3)-O(31). With all diacyl

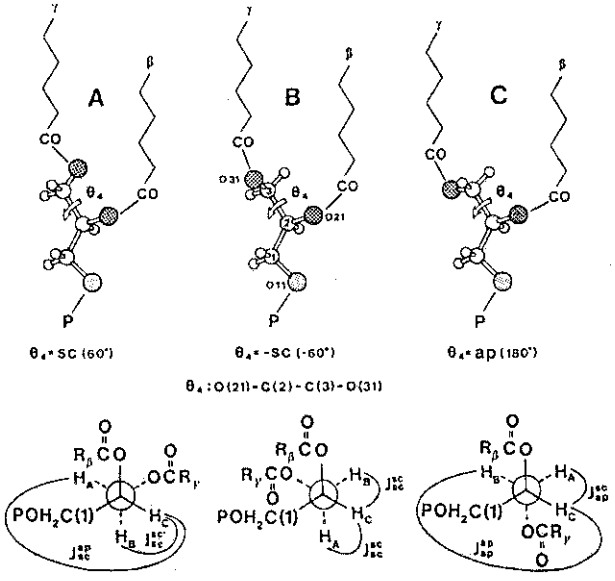

Fig. 8. The three energetically favored conformations A, B and C of the glycerol C(2)-C(3) bond of phospholipids. For atom numbering and notation of torsion angles see Fig. 5. The three rotamers A, B and C are characterized by two related torsion angles θ_3 = C(1)-C(2)-C(3)-O(31) and θ_4 = O(21)-C(2)-C(3)-O(31). The torsion angle θ_4 determines the relative orientation of the two ester oxygen atoms O(21) and O(31) attached to glycerol C(2) and C(3), respectively. In rotamers A and B torsion angle θ_4 is ± synclinal (sc) and these two rotamers are referred to as sc or gauche rotamers. In rotamer C, the value of θ_4 is antiperiplanar (ap) and this rotamer is referred to as ap rotamer. The polar group is attached to O11 (stippled) pointing downward. The asymmetric C(2) glycerol atom has the natural D configuration. Newman projections of rotamers A, B and C are included (bottom) and so are the component vicinal ^{1}H spin coupling constants *J* used to derive fractional rotamer populations expressed as % summarized in Table 4. For values of the component coupling constants see [20].

phospholipids listed in Table 4, the C(3)H_2 glycerol protons give rise to an eight-line spectrum of an ABX spin system indicating that these two glycerol protons are both chemically and magnetically non-equivalent. The following conclusions can be derived from the ^{1}H high-resolution NMR studies [4,20, 22].

(I) The spectral properties of the glycerol C(3)H_2 group are consistent with a preferred conformation about the C(2)-C(3) glycerol bond.

(II) There are two preferred conformations about this glycerol bond. The dominant conformation is characterized by torsion angles θ_3 = ap, θ_4 = +sc (rotamer A, Fig. 8) and the other one by θ_3 = +sc and θ_4 = −sc (rotamer B, Fig. 8). In both rotamers A and B the two ester oxygens O(21) and O(31), attached to glycerol C(2) and C(3), respectively, are synclinal. Studies using molecular models show that only in these two rotamers with $\theta_4 = \pm$ sc are the ester oxygens O(21) and O(31) in close proximity to allow for parallel stacking of the two hydrocarbon chains. The ratio of rotamers A and B that exist in dynamic equilibrium (see below) ranges from 1 to 2.

(III) In micelles of short-chain phospholipids the diacylglycerol part fluctuates between two energetically favorable conformations (rotamers A and B). These fluctuations or motional averaging are fast on the NMR time scale and are necessarily coupled to appropriate changes in torsion angles β_1 to β_4 and γ_1 to γ_4 (cf. Fig. 5) of the β- and γ-hydrocarbon chains, respectively, as indicated in Fig. 9.

(IV) In rotamer C with θ_3/θ_4 = −sc/ap the conformation of the two ester oxygens O(21) and O(31) is ap and as a result the two hydrocarbon chains extend in opposite directions preventing parallel chain stacking (Fig. 8). This rotamer is therefore energetically unfavorable and, indeed, rotamer C is practically absent in micelles (cf. Table 4).

(V) At concentrations below the cmc, i.e. in the monomeric state, rotamer C is present though its contribution is usually less than 10% for ester phospholipids. It follows that the parallel alignment of the two hydrocarbon chains is largely maintained even in the monomeric state (cf. Table 4).

(VI) The nature of the solvent (dielectric) has little effect on the distribution of rotamers (cf. Table 4). In both water and organic solvent rotamers A and B are predominant.

(VII) Apparently parallel chain stacking in phospholipid aggregates (micelles, bilayers) governs the preferred conformation about the C(2)-C(3) glycerol bond.

Table 4
Preferred conformation of the C(2)-C(3) glycerol bond of short-chain phospholipids

Compound	Vicinal spin[a] coupling constant (Hz)		Rotamer population (%)			Experimental conditions
	$^3J_{AC}$	$^3J_{BC}$	A	B	C	
2,3-Dihexanoyl-D-glycero-1-phosphocholine	7.6	2.4	62	38	1	in ^2H_2O, > cmc
	6.8	3.0	52	42	6	in ^2H_2O, < cmc
2,3-Dihexanoyl-D-glycero-1-phosphoethanolamine	7.7	2.3	63	37	1	in ^2H_2O, pH 6.0, > cmc
	7.9	1.8	68	32	0	in ^2H_2O, pH 9.3, > cmc
	7.2	3.1	55	38	7.5	in ^2H_2O, pH 6.0, < cmc
2,3-Di-*O*-hexyl-D-glycero-1-phosphocholine	6.5	3.0	49	44	6.5	in ^2H_2O, > cmc
	5.6–6.5	3.3–3.8	38–48	42–47	10–16	in ^2H_2O, pH 6.0, < cmc
2,3-Dihexanoyl-D-glycero-1-phospho-L-serine ammonium salt	7.6	2.4	62	38	1	in ^2H_2O, > cmc
	7.1	3.0	55	39	6.5	in ^2H_2O, < cmc
2,3-Dipalmitoyl-DL-glycero-1-phosphocholine	6.9	3.1	52	40	7.5	in $C^2HCl_3/C^2H_3O^2H$, 2:1 (v/v)
2,3-Dipalmitoyl-DL-glycero-1-phosphoethanolamine	6.9	3.4	51	38	11	in $C^2HCl_3/C^2H_3O^2H$, 2:1 (v/v)
2,3-Dipalmitoyl-D-glycero-1-phospho-L-serine	7.2	3.0	55	38	6.5	in $C^2HCl_3/C^2H_3O^2H$, 4:3 (v/v)

The three staggered conformations of minimum free energy, rotamers A–C, are shown in Fig. 8.
[a]The lettering of the glycerol protons is defined in Table 2.

4.3. Comparison of the motionally averaged conformation of short-chain phospholipids with single-crystal structures of lipids

The NMR results discussed above are supported by X-ray crystallography. In all single-crystal structures of diacyl phospholipids and glycosphingolipids available to date the torsion angle $\theta_4 = \pm$ sc. In these crystal structures conformations A and B (Fig. 8) are observed exclusively consistent with parallel chain stacking. In Fig. 9 four representative single-crystal structures of diacyl phospholipids are depicted which differ in torsion angle θ_4 and in details of the chain stacking and the orientation of the glycerol group with respect to the bilayer normal. The two structures on the left, DMPCA (top) and DLPA (bottom), have conformation A (θ_3 = ap, θ_4 = sc) and the two on the right, $DLPEM_2$ (top) and DMPGA (bottom), have conformation B (θ_3 = sc, $\theta_4 = -$sc) (cf. Figs. 8 and 9). There are two types of rotamers A (Aβ, Aγ) and B (Bβ, Bγ) which differ in the chain stacking mode. In rotamers Aγ (DMPCA) and Bγ ($DLPEM_2$) the γ-chain extends in a straight zigzag from the glycerol backbone while the β-chain is initially at a right angle to the γ-chain and adopts a parallel alignment to the γ-chain by a 90° bend at its second C-atom (cf. Fig. 9 top, DMPCA and $DLPEM_2$). In rotamers Aβ and Bβ the β-chain is straight and the γ-chain is initially horizontal and gets aligned with the β-chain by a 90° bend at C-atom 2 (cf. Fig. 9 bottom, DLPA and DMPGA). Fig. 9 describes possible interconversions of the four different single-crystal structures and defines the sum of operations required to accomplish these interconversions. For instance, the conversion of structure Aγ to Bγ involves not only a change in θ_3 from ap to +sc and θ_4 from sc to −sc, but simultaneous changes in torsion angles γ_1, β_1, β_3 and β_4 (marked by small circular arrows in Aγ, Fig. 9). Fig. 9 illustrates that a conformational change about the C(2)-C(3) glycerol bond, i.e. a change in torsion angles θ_3 and θ_4, is accompanied by appropriate changes in the torsion angles of adjacent bonds in the hydrocarbon chains so that the hydrocarbon chain stacking is maintained.

The knowledge of the structure and dynamics of the diglyceride part of short-chain PC molecules is crucial for an understanding of the function of these

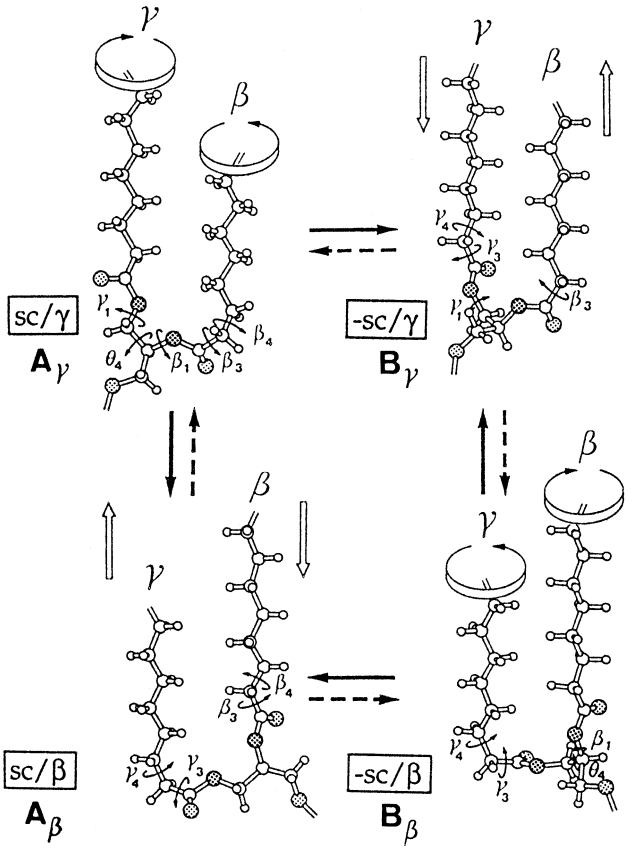

Fig. 9. Four preferred conformations of the C(2)-C(3) glycerol bond observed in different single-crystal structures of diacyl phospholipids. The four single-crystal structures are DMPCA (top left), $DLPEM_2$ (top right), DLPA (bottom left) and DMPGA (bottom right). These four crystal structures differ not only in the conformation of the glycerol C(2)-C(3) bond, but also in the chain stacking mode and the orientation of the glycerol group with respect to the bilayer plane. Bold letters A and B refer to different conformations of the glycerol C(2)-C(3) bond as defined in Fig. 8. Conformer A: θ_3 = ap, θ_4 = sc; conformer B: θ_3 = sc, $\theta_4 = -$sc. The interconversion of the four single-crystal structures is indicated by heavy arrows and the reversible character of these interconversions by the dashed arrows. The interconversions along the horizontal heavy arrows involve primarily a conformational change about the C(2)-C(3) glycerol bond, those along vertical arrows mainly changes in the chain stacking mode with the conformation about the C(2)-C(3) bond and thus torsion angles θ_3/θ_4 remaining unchanged. For instance, the sum of the conformational changes involved in the conversion of Aγ to Bγ are indicated by large and small circular arrows; the large circular arrows indicate 120° rotations of the total hydrocarbon chains, the small circular arrows mark conformational changes in single bonds. For details the reader is referred to the original literature [11,12].

molecules. From high-resolution NMR it is clear that short-chain phospholipid molecules in micelles undergo conformational changes between rotamers A and B. The interconversion rate is apparently fast on the NMR time scale. The purpose of considering different single-crystal structures of phospholipids as minimum free energy conformations is to demonstrate that a conformational change in the C(2)-C(3) glycerol bond, i.e., the interconversion of rotamers A to B, must be accompanied by conformational changes of adjacent bonds in the hydrocarbon chains so that the parallel alignment of the two hydrocarbon chains is preserved. The sum of these conformational changes manifests itself in changes in the chain stacking mode and changes in the orientation of the glycerol group. For instance, the orientation of the glycerol group is parallel to the bilayer plane in the Aβ structure (see DLPA, Fig. 9) and changes to a perpendicular orientation upon conversion to the Aγ structure (see DMPCA, Fig. 9). The motionally averaged conformation of the diacylglycerol part of short-chain phospholipids in micelles may be regarded as an average of the four different conformations presented in Fig. 9. The weighting factor and hence the relative probabilities of the four conformations are still unknown, what is known from NMR studies is that populations Aβ and Aγ are dominant, with the population ratio A/B ranging from 1 to 2 (cf. Table 4).

5. Detergent properties of short-chain phosphatidylcholines

Gabriel and Roberts [26] were the first to point out the dispersing action of short-chain phospholipids. These authors concluded from high-resolution NMR measurements that unilamellar vesicles form spontaneously upon mixing of aqueous dispersions of long-chain and short-chain PC. Spontaneous formation of vesicles was reported for long-chain PC of 14 or more C-atoms containing saturated or unsaturated hydrocarbon chains when mixed with diC_6PC, diC_7PC or diC_8PC at a molar ratio of long-chain PC/short-chain PC of about 4:1. The same final product is obtained when for instance $diC_{16}PC$ and the short-chain PC are dissolved in organic solvent in a 4:1 molar ratio, the solvent is removed by evaporation and the dry lipid film rehydrated and dispersed in an aqueous solvent [26].

Mixed dispersions of 20 mM $diC_{16}PC$ and 5 mM diC_7PC give similar ^1H high-resolution NMR spectra regardless which of the two methods of mixing is used. The resulting dispersion is opalescent, quite different in appearance from the milky white suspension of pure $diC_{16}PC$ in which the phospholipid is present as large, multilamellar vesicles. The latter structures are known to give very broad unresolved ^1H-NMR spectra. Upon addition of 5 mM diC_7PC to a dispersion of multilamellar $diC_{16}PC$ vesicles (20 mM) at 25°C, high-resolution spectral features appear within 5 min of mixing. The initially still broad resonances narrow with a half-time of about 1 h reaching a thermodynamically stable or at least metastable state after about 8 h. These observations are a clear demonstration of the dispersing, detergent-like effect of short-chain PC [26].

The resulting lipid aggregate or phase present in mixed dispersions of long-chain PC and short-chain PC was investigated by the same authors using different methods including NMR, FTIR, fluorescence spectroscopy, DSC and electron microscopy [27]. From a combination of ^1H- and ^{31}P-NMR measurements, electron microscopy of negatively stained samples and DSC the particles present in dispersions of mixtures of long-chain PC and short-chain PC (molar ratio 4:1) were identified as unilamellar vesicles. Convincing evidence for the presence of unilamellar vesicles was provided by ^1H- and ^{31}P-NMR signal intensity and line width measurements, by ^1H spin-lattice relaxation time T_1 measurements and the use of lanthanide shift reagents [26,27].

From a comparison of the ^1H spin-lattice relaxation time T_1 values for diC_7PC in pure diC_7PC micelles with T_1 values measured for both $diC_{16}PC$ and diC_7PC in a 4:1 mixture [26], the authors inferred the presence of vesicles. Consistent with this interpretation are shift changes in the ^1H-NMR spectrum induced by the addition of lanthanide shift reagents. In the presence of Pr^{3+} only part of the $-N(CH_3)_3$ resonance is shifted downfield and this part is assigned to PC molecules located on the outer leaflet of the vesicle bilayer and hence exposed to Pr^{3+}. The unshifted part of the $-N(CH_3)_3$ signal arises from lipid molecules forming the inner leaflet of the bilayer. The NMR results discussed above are taken together

as evidence that short-chain PC induce vesiculation in multibilayers of long-chain PC resulting in a sizable population of unilamellar vesicles. What remains unclear is if and to what extent mixed micelles are present in these lipid mixtures.

The size distribution of unilamellar vesicles formed from $diC_{16}PC$ and a short-chain PC (diC_6PC, diC_7PC or diC_8PC) ranges from 17 to 40 nm as determined by electron microscopy [27]. The phase of the long-chain phospholipid appears to affect the average size of the resulting vesicles. Small unilamellar vesicles result when short-chain PC are mixed with long-chain phospholipids in the gel state, as is the case when $diC_{16}PC$, $diC_{18}PC$, and sphingomyelin dispersions are mixed with short-chain phospholipids at room temperature. The average diameter of vesicles consisting of one of these long-chain phospholipids (20 mM) mixed with diC_7PC (5 mM) at room temperature are 17 ± 5 nm, 16 ± 5 nm and 15 ± 7 nm, respectively [27]. In contrast, if short-chain PC are mixed with long-chain phospholipids in the liquid-crystalline state larger vesicles are obtained which frequently contain residual multilamellar structures [27]. Mixing of diC_7PC (5 mM) with $diC_{14}PC$ or egg PC (20 mM) which are liquid-crystalline at room temperature yields unilamellar vesicles of an average diameter of 28 ± 5 nm and 83 ± 85 nm, respectively [27].

DSC experiments support the conclusions drawn from NMR and electron microscopy studies. As shown in Fig. 10 a mixture of 20 mM $diC_{16}PC$ and 5mM diC_8PC undergoes a gel-to-liquid crystal phase transition that closely resembles that observed with small unilamellar $diC_{16}PC$ vesicles produced by sonication. For both sonicated $diC_{16}PC$ vesicles and the $diC_{16}PC/diC_8PC$ mixture broad phase transitions are observed with lower phase transition temperatures and enthalpies (areas under the peak) compared to the transition of an unsonicated dispersion of multilamellar $diC_{16}PC$ structures (cf. heating curves A to C in Fig. 10) [27]. Sometimes two transitions are observed with mixtures of long-chain and short-chain PC indicating that the long-chain PC is present in two different environments (cf. Fig. 10C). The DSC results obtained with mixtures of long-chain and short-chain PC are incompatible with the presence of residual large multilamellar structures. They are consistent with dispersed structures be it

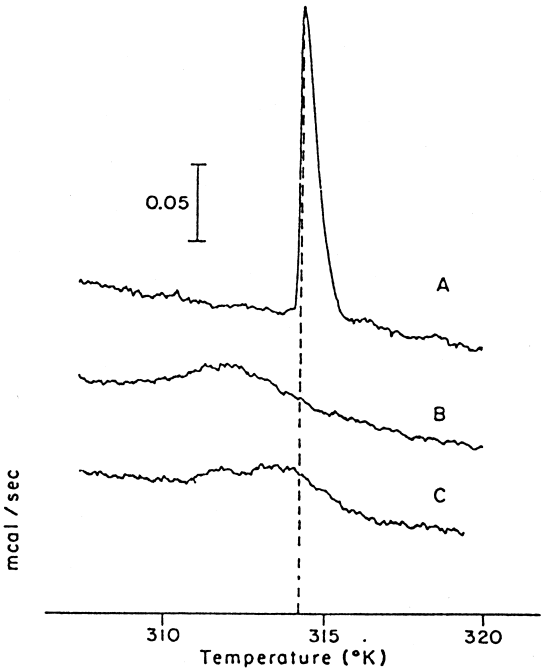

Fig. 10. Initial DSC heating curves of an unsonicated dispersion of 20 mM $diC_{16}PC$ in 0.15 M NaCl pH $\approx$ 7 (A), the same dispersion as in A after sonication to produce SUV (B), and a dispersion consisting of 20 mM $diC_{16}PC$ and 5 mM diC_8PC dispersed in phosphate-buffered 0.2 M KSCN solution pH 7.0 (C) (from [27]).

small unilamellar vesicles or disc-shaped micelles [27].

The stability of the unilamellar vesicles present in mixtures of long-chain and short-chain PC can be readily monitored by encapsulating the fluorescent dye 6-carboxyfluorescein and measuring the time course of the fluorescence intensity [26]. These measurements indicate that the size of the vesicles remain unchanged for days to one week and the same is true for the bilayer permeability of these vesicles [26]. The vesicles are potentially useful for membrane protein reconstitution and drug encapsulation, applications that require stable, nonleaky vesicles.

6. Interaction of short-chain phospholipids with biological membranes

6.1. Solubilization of integral membrane proteins with short-chain PC

Further evidence for the dispersing power of short-

chain PC was provided by Kessi et al. [30]. DiC_7PC was shown to solubilize both plasma membranes such as for example brush border membrane vesicles (BBMV) and erythrocyte ghosts, and organelle membranes, e.g., rat liver mitochondria and chromatophore membranes prepared from *Rhodospirillum rubrum*. Typically S-shaped solubilization curves are obtained plotting the percentage of solubilized protein as a function of the total diC_7PC concentration or the diC_7PC/protein weight ratio (Fig. 11). With organelle membranes lacking a cytoskeleton 85–95% of the membrane proteins are solubilized at [diC_7PC] > 10–20 mM (diC_7PC/protein weight ratio 1–2) (Table 5). The protein yield is significantly reduced with plasma membranes, 65–80% for BBM and 40–45% for erythrocyte ghosts. Plasma membranes can be solubilized to a similar extent as organelle membranes after removal of cytoskeletal proteins, e.g., erythrocyte ghosts are solubilized to approx. 80% after removal or disruption of the cytoskeleton (Table 5). By normalizing, i.e., plotting the percentage of solubilized protein as a function of the diC_7PC/protein weight ratio rather than diC_7PC concentration, all data points for a particular membrane obtained at different protein concentrations come to lie on a single S-shaped curve (Fig. 11B). This result indicates that a particular membrane is solubilized at a constant diC_7PC/protein weight ratio (Table 5).

The original membrane particles used in the study of Kessi et al. [30] range widely in size from approx. 50 nm for chromatophores to approx. 7000 nm for erythrocyte ghosts. Solubilization of these membrane particles in excess diC_7PC produces small mixed micelles consisting of membrane protein, membrane lipids and diC_7PC. The size distribution of the mixed micelles exhibits well defined maxima at about 10 nm as demonstrated by gel filtration on Sepharose Cl-4B and freeze-fracture EM. The marked difference in size between the original and solubilized membrane particles is good evidence for the effective solubiliza-

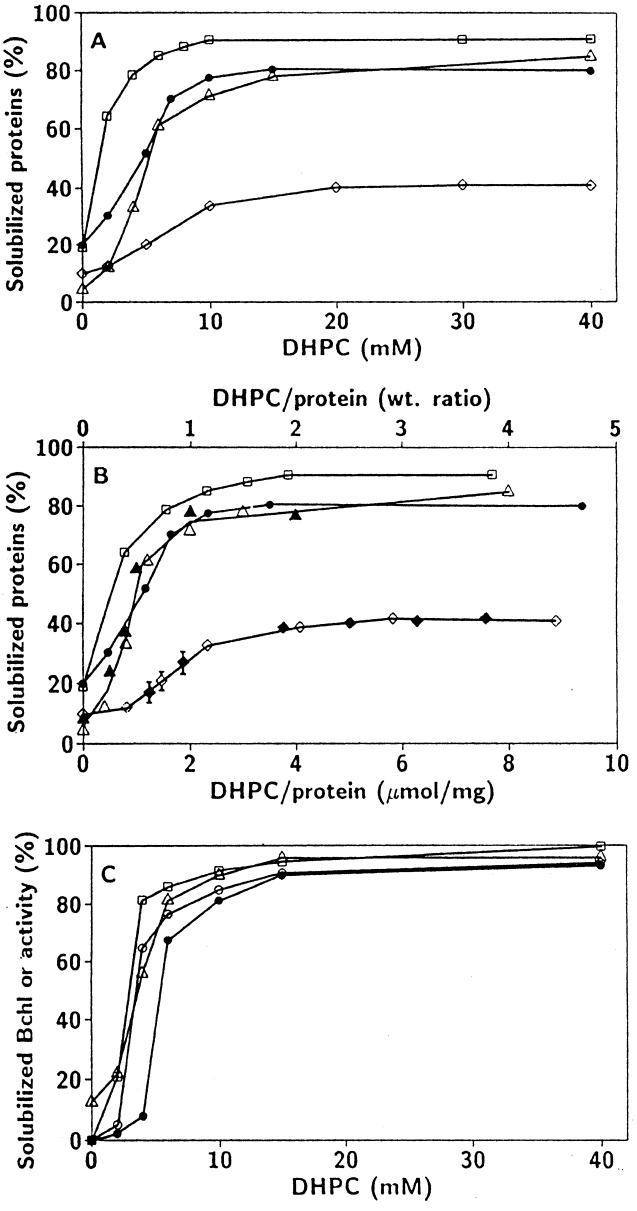

Fig. 11. Solubilization of plasma and organelle membranes by diC_7PC. (A) Solubilization expressed as % of different membranes as a function of the total diC_7PC concentration. ●, BBMV at 4.3 mg of protein/ml; ◇, erythrocyte ghosts at 4.5 mg of protein/ml; △, chromatophores from *R. rubrum* at 5.0 mg of protein/ml; □, mitochondria at 2.6 mg of protein/ml. For experimental details see [30]. In the normalized plots of panel B the solubilization curves are independent of protein concentration as shown for chromatophores from *R. rubrum* at 10 mg of protein/ml (▲) and 5 mg/ml (△) and erythrocyte ghosts at 4.5 mg/ml (◇) and 1.6 mg/ml (◆); mitochondria at 2.6 mg protein/ml (□), BBM vesicles at 4.3 mg protein/ml (●). (C) Solubilization curves of various proteins of chromatophores from *R. rubrum* in the presence of diC_7PC at 0°C. The membranes were suspended in 10 mM Tris-HCl buffer pH 7.5, 0.15 M NaCl and 2 mM $MgCl_2$ and solubilized as described above. The protein concentration was between 4.8 and 5.2 mg/ml. □, adenosine triphosphate (ATPase); ○, succinate dehydrogenase; △, NADH dehydrogenase; ●, bacteriochlorophyll-containing proteins. Adapted from Kessi et al. [30]. DHPC = diC_7PC

Table 5
Solubilization of plasma and organelle membranes by diC_7PC

Plasma membrane	Organelle membrane	Lipid/protein weight ratio in intact membrane	diC_7PC/protein weight ratio[a]	Amount of protein (%) solubilized at 40 mM diC_7PC[b]
Erythrocyte ghosts		0.8	0.75 ± 0.05	43 ± 3 (80 ± 5)
Brush border membrane		0.5	0.45 ± 0.05	73 ± 7
	chromatophores	0.5	0.45 ± 0.05	85 ± 5
	mitochondria	0.3	0.26 ± 0.05	93 ± 3

[a]This is the diC_7PC/protein weight ratio taken at the inflection point of the normalized S-shaped curves in Fig. 11B.
[b]Solubilization of membrane proteins at 40 mM diC_7PC. Erythrocyte ghosts were solubilized to 80% (value in parentheses) after removal of the cytoskeleton [30].

tion of both plasma and organelle membranes. Furthermore, BBMV are solubilized at a diC_7PC concentration of 15 mM and a diC_7PC/protein weight ratio of 1.6 (Fig. 11A,B). For comparison, the values of the detergent/protein weight ratio for the solubilization of BBMV with Triton X-100 and sodium cholate are increased to 5 and 10, i.e., by a factor of 3 and 6, respectively. These results are convincing evidence for the superior dispersing power of short-chain PC.

Important features of the solubilization of biological membranes by excess short-chain PC are (I) the preservation of the native conformation and hence the activity of the solubilized membrane proteins. There is ample evidence showing that different enzymes solubilized from different membranes, e.g., chromatophores (Table 6), intestinal BBM, renal medulla membrane [30], all retain their activity in the solubilized state. (II) The activity of membrane proteins is not only retained at diC_7PC concentrations of 10–20 mM at which maximum solubilization occurs, but also in a 4–5-fold excess of diC_7PC (Table 6). This appears to be an important characteristic of short-chain PC [30].

By comparison with the performance of other detergents widely used in membrane solubilization/reconstitution, Kessi et al. [30] concluded that short-chain PC are superior to most other detergents. Short-chain PC as detergents have some advantageous properties such as their availability as highly purified compounds, their electroneutrality and stability over a wide pH range. Another feature, probably more important in membrane solubilization/reconstitution, is evident from an inspection of Table 5. Apparently the diC_7PC/protein weight ratio at the point of solubilization (derived from the inflexion point of the S-shaped curves of Fig. 11B) represents a characteristic value for each biological membrane (cf. Table 5). There is a striking correlation between this weight ratio and the intrinsic lipid/protein weight ratio of the original membrane (cf. columns 3 and 4 of Table 5). Such a correlation is expected if diC_7PC distributes primarily into the lipid bilayer of the biological membrane and its interaction with membrane proteins is weak. The observation that enzymatic activities are retained over a large concentration range of diC_7PC supports this notion (Table 6).

Table 6
Activities of various proteins of chromatophore membranes of *R. rubrum* $G9^+$ in the presence of diC_7PC[a]

Protein	[diC_7PC] (mM)					
	2	4	6	10	15	40
ATPase	164	164	150	153	164	170
NADH dehydrogenase	175	211	194	199	198	210
Succinate dehydrogenase	60	60	64	66	69	70
Reaction center	–	–	–	–	–	105

[a]Activities are expressed as % of the activity observed in native chromatophore membranes, i.e., in the absence of diC_7PC. Adapted from [30].

Kessi et al. [30] proposed the following mechanism of membrane solubilization: when diC_7PC as a wedge-shaped molecule is inserted into the external leaflet of the membrane, considerable tension between the two membrane leaflets is generated leading to the destabilization and eventually to the solubilization of the membrane. The resulting disc-shaped micelles are unstable due to the exposure to water of the hydrocarbon chains of those membrane lipid molecules located along the circumference of the disc-shaped micelle. Short-chain PC appears to be structurally well suited to interact preferentially with the hydrocarbon chains of lipids located at the edge of the disc-shaped micelles thus shielding these hydrocarbon chains from the energetically unfavorable contact with water. Short-chain PC molecules seem to have two complementary activities: first, they exert a dispersing effect on lipid bilayers, and second, in the process of membrane disintegration they apparently stabilize the micelles in statu nascendi. Obviously the sum of these two activities is responsible for the effective solubilization of biological membranes and the subsequent stabilization of the mixed protein/lipid micelles. The retention of the native protein structure in the solubilized micellar state is therefore a consequence of the weak interaction or the lack of interaction of short-chain PC with membrane proteins. The direct interaction of short-chain PC with an integral membrane protein thereby displacing an intrinsic membrane lipid from the protein-lipid interface seems to be unlikely. Consequently after solubilization of biological membranes with short-chain PC, integral membrane proteins remain in their natural environment of intrinsic membrane lipids. The native conformation and enzymatic activity are effectively preserved.

6.2. *Reconstitution of simple artificial membrane systems (proteoliposomes) using short-chain PC*

Kessi et al. [30] reported that short-chain PC lend themselves very well not only to membrane solubilization, but also to the reconstitution of the solubilized membrane proteins to simple artificial membrane systems (proteoliposomes). These authors reported the solubilization and purification of sucrase-isomaltase from small-intestinal BBM using DiC_7PC and the reconstitution of this protein. Furthermore, the first successful solubilization and reconstitution of the Na^+-dependent D-glucose transporter of the small-intestinal BBM was accomplished with diC_7PC. The resulting reconstituted system exhibited a statistically significant D-glucose overshoot. Boffelli et al. [31] succeeded in solubilizing and reconstituting scavenger receptor class B type I (SR-BI) of the small intestinal BBM. The resulting artificial membrane system closely resembled in its activity the original BBMV used as a starting material.

A large body of literature exists on the solubilization and reconstitution of Ca^{2+}-ATPase from skeletal muscle sarcoplasmic reticulum. A number of different detergents have been used with varied success including bile salts [32–34], Triton X-100 [34,35], octylglucoside [34] and poly(oxyethylene)-8-lauryl ether ($C_{12}E_8$) [34,36,37]. These studies clearly show that the detergent is crucial in the solubilization/reconstitution process determining the recovery of activity. Among the detergents used in the above studies, $C_{12}E_8$ proved to be best in preserving the native conformation and biological function of the Ca^{2+}-ATPase. In a more recent comparative study Shivanna and Rowe [38] assessed the performance of cholate, deoxycholate, $C_{12}E_8$ and diC_7PC in solubilizing/reconstituting Ca^{2+}-ATPase from sarcoplasmic reticulum. As shown in Fig. 12, significantly more Ca^{2+}-ATPase activity is solubilized by diC_7PC over a wide range of diC_7PC concentrations than by $C_{12}E_8$ or bile salts. Furthermore the specific activity of the diC_7PC-solubilized Ca^{2+}-ATPase is significantly greater than that solubilized by any of the other three detergents. There is a broad range of optimum diC_7PC concentrations whereas the other detergents exhibit a well defined peak in the specific activity vs. detergent concentration plot (Fig. 12C). Above this optimum detergent concentration the specific activity of the solubilized Ca^{2+}-ATPase decreases significantly with increasing detergent concentration. Purification of the detergent-solubilized Ca^{2+}-ATPase on a sucrose gradient confirms the result of Fig. 12: diC_7PC is superior to $C_{12}E_8$ and the bile salts in terms of protein yield and the recovery of total and specific activity. The coupling of Ca^{2+} transport and ATP hydrolysis in the diC_7PC-purified Ca^{2+}-ATPase is maximal matching the values obtained with native sarcoplasmic reticulum. Similarly, the specific activity of Ca^{2+}-ATPase reconstituted into dioleoyl PC

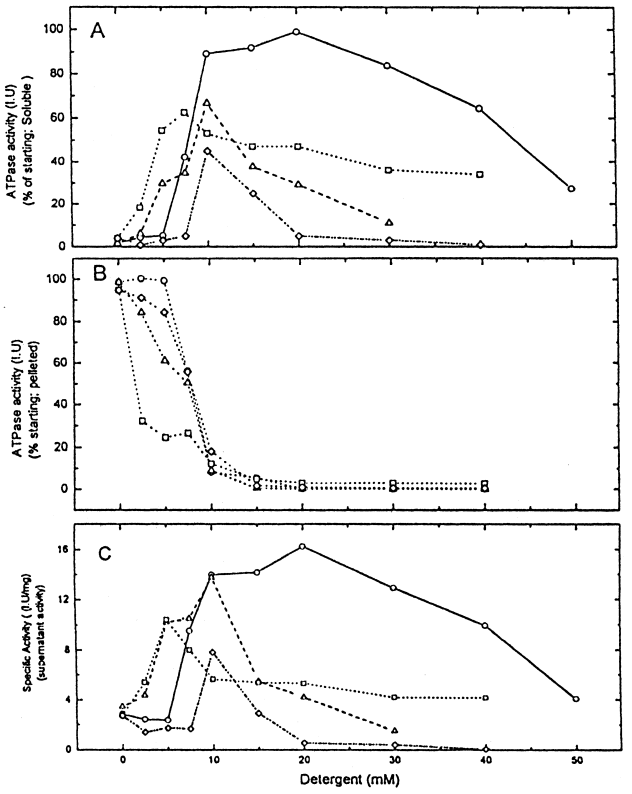

Fig. 12. Solubilization of sarcoplasmic reticulum Ca^{2+}-ATPase by diC_7PC, sodium cholate, sodium deoxycholate and $C_{12}E_8$. (A) Total activity of Ca^{2+}-ATPase recovered in the supernatant; (B) total activity of Ca^{2+}-ATPase in the pellet; (C) specific activity of solubilized Ca^{2+}-ATPase recovered in mixed detergent micelles. Total activities are expressed as percentage of starting material. Specific activity (C) is in units of ATPase activity/min per mg of protein at 37°C determined under standard assay conditions as described in [38]. ○, DiC_7PC; △, $C_{12}E_8$; □, Na^+ cholate; ◇, Na^+ deoxycholate.

vesicles using diC_7PC is similar to that measured in native sarcoplasmic reticulum. It is greater by a factor of 2 compared to the specific activity of Ca^{2+}-ATPase reconstituted with $C_{12}E_8$ [38].

This study clearly shows that diC_7PC is an excellent detergent for the solubilization, purification and reconstitution of Ca^{2+}-ATPase from sarcoplasmic reticulum. It is superior to any other previously used detergent in terms of Ca^{2+}-ATPase yield and recovery of specific activity [38] confirming the conclusions of Kessi et al. [30]. A similar mechanism of solubilization was proposed by Shivanna and Rowe [38]: the interaction of diC_7PC with Ca^{2+}-ATPase is presumably weak and short-chain PC are therefore unlikely to displace intrinsic membrane lipids. This behavior is contrasted by $C_{12}E_8$ which was shown to displace intrinsic, natural lipids from the Ca^{2+}-ATPase-lipid interface [39], a process that is accompanied by loss of enzymatic activity.

7. Miscellaneous applications of short-chain phospholipids

Mixed micelles resulting from the solubilization of biological membranes have been used to enrich and/or purify integral membrane proteins. In addition to the purification of diC_7PC-solubilized sucrase-isomaltase and Ca^{2+}-ATPase mentioned above, the partial purification of retinyl ester synthetase and retinoid isomerase from bovine ocular pigment epithelium was reported [40]. Furthermore, the purification of bacteriochlorophyll-binding proteins solubilized with diC_7PC from chromatophores of *R. rubrum* was described yielding a protein complex consisting of light-harvesting complex I and reaction center [41].

Several detergents including short-chain phospholipids were reported to promote the orientation of liquid-crystalline 1,2-$diC_{14}PC$ bilayers in a magnetic field [42–44]. Magnetic orientation of mixed lipid-detergent micelles containing macromolecules such as integral and peripheral membrane proteins has been employed with the aim of applying solid state and high-resolution NMR methods and deriving conformational and dynamic information on membrane proteins. The ideal mixed micelle in which the protein is dispersed should satisfy the following criteria: first, it should provide an environment which is close to the natural one so that the native protein structure and the enzymatic activity are preserved, and second, the tumbling of the micellar complex should be sufficiently fast to yield highly resolved NMR spectra.

From the discussion above it is expected that mixtures of $diC_{14}PC$ and diC_6PC form lipid bilayer discs edge-stabilized by diC_6PC. This is borne out by experiment at $diC_{14}PC/diC_6PC$ molar ratios ranging from 1.5:1 to 4:1 [45,46]. At 25% total lipid concentration these bilayer discs can be oriented in the magnetic field at $diC_{14}PC/diC_6PC$ molar ratios ranging from 2:1 to 3.5:1. Sanders and Landis [47] assembled integral and peripheral membrane proteins into $diC_{14}PC/diC_6PC$ discoidal micelles and after aligning

them in the magnetic field assessed their usefulness for NMR structural studies. The results vary widely, some of the assemblies thus produced give well resolved NMR spectra [45]. The real potential of this methodology in terms of structure elucidation of integral membrane proteins is still unclear.

Short-chain phospholipids have also been applied successfully to the crystallization of membrane proteins. Porin, an integral membrane protein of the outer membrane of *Escherichia coli*, was crystallized in the sole presence of diC_6PC [48]. Crystals were obtained which diffracted X-rays to 3.5 Å resolution, and the crystal morphology and unit cell dimensions were the same as those obtained with detergent-grown crystals.

The list of useful applications of short-chain phosphatidylcholines as mild detergent-like compounds can be expected to increase in the future. It will be interesting to compare the physico-chemical properties of the isoelectric short-chain phosphatidylcholines with those of negatively charged short-chain phospholipids such as diC_6 phosphatidylserines, and study the behavior of this class of short-chain phospholipids in membrane solubilization and reconstitution.

References

[1] R.J.M. Tausk, J. Karmiggelt, C. Oudshoorn, J.Th.G. Overbeek, Biophys. Chem. 1 (1974) 175–183.
[2] G.H. De Haas, P.P.M. Bonsen, W.A. Pieterson, L.L.M. van Deenen, Biochim. Biophys. Acta 239 (1971) 252–260.
[3] R.E. Jonson, M.A. Wells, J.A. Rupley, Biochemistry 20 (1981) 4239–4242.
[4] H. Hauser, W. Guyer, I. Pascher, P. Skrabal, S. Sundell, Biochemistry 19 (1980) 366–373.
[5] O.A. Roholt, M. Schlamowitz, Arch. Biochem. Biophys. 94 (1961) 364–386.
[6] P.P.M. Bonsen, G.H. de Haas, W.A. Pieterson, L.L.M. van Deenen, Biochim. Biophys. Acta 270 (1972) 364–382.
[7] T. Lin, S. Chen, N.E. Gabriel, M.F. Roberts, J. Am. Chem. Soc. 108 (1986) 3499–3507.
[8] R. Smith, C. Tanford, J. Mol. Biol. 67 (1972) 75–83.
[9] R.J.M. Tausk, J. van Esch, J. Karmiggelt, G. Voordouw, J.Th.G. Overbeek, Biophys. Chem. 1 (1974) 184–203.
[10] R.J.M. Tausk, C. Oudshoorn, J.Th.G. Oberbeek, Biophys. Chem. 2 (1974) 53–63.
[11] H. Hauser, I. Pascher, R.H. Pearson, S. Sundell, Biochim. Biophys. Acta 650 (1981) 21–51.
[12] I. Pascher, M. Lundmark, P. Nyholm, S. Sundell, Biochim. Biophys. Acta 1113 (1992) 339–373.
[13] N.P. Franks, J. Mol. Biol. 100 (1976) 345–358.
[14] J. Seelig, H.-U. Gally, R. Wohlgemuth, Biochim. Biophys. Acta 467 (1977) 109–119.
[15] G. Büldt, H.-U. Gally, A. Seelig, J. Seelig, G. Zaccai, Nature 271 (1978) 182–184.
[16] G. Büldt, H.-U. Gally, J. Seelig, G. Zaccai, J. Mol. Biol. 134 (1979) 673–691.
[17] R.D. Hershberg, G.H. Reed, A.J. Slotboom, G.H. de Haas, Biochim. Biophys. Acta 424 (1976) 73–81.
[18] M.F. Roberts, A.A. Bothner-By, E.A. Dennis, Biochemistry 17 (1978) 935–942.
[19] H. Hauser, W. Guyer, P. Skrabal, FEBS 11th Meeting Copenhagen 1977, vol. 46, Symposium A5, 1978, pp. 73–82.
[20] H. Hauser, I. Pascher, S. Sundell, Biochemistry 27 (1988) 9166–9174.
[21] C. Zhou, V. Garigapati, M.F. Roberts, Biochemistry 36 (1997) 15925–15931.
[22] S.F. Martin, G.E. Pitzer, Biochim. Biophys. Acta 1464 (2000) 104–112.
[23] C.F. Schmidt, Y. Barenholz, C. Huang, T.E. Thompson, Biochemistry 16 (1977) 3948–3954.
[24] R.A. Burns Jr., M.F. Roberts, Biochemistry 19 (1980) 3100–3106.
[25] M.F. Brown, J. Seelig, U. Häberlen, J. Chem. Phys. 70 (1979) 5045–5053.
[26] N.E. Gabriel, M.F. Roberts, Biochemistry 23 (1984) 4011–4015.
[27] N.E. Gabriel, M.F. Roberts, Biochemistry 25 (1986) 2812–2821.
[28] M. Sundaralingam, Ann. NY Acad. Sci. 195 (1972) 324–355.
[29] W. Klyne, V. Prelog, Experientia 16 (1960) 521–523.
[30] J. Kessi, J.-C. Poirée, E. Wehrli, R. Bachofen, G. Semenza, H. Hauser, Biochemistry 33 (1994) 10825–10836.
[31] D. Boffelli, F.E. Weber, S. Compassi, M. Werder, G. Schulthess, H. Hauser, Biochemistry 36 (1997) 10784–10792.
[32] F. Michelangeli, F.M. Munkonge, Anal. Biochem. 194 (1991) 231–236.
[33] G. Szymanska, H.W. Kim, E.G. Kranias, Biochim. Biophys. Acta 1091 (1991) 127–134.
[34] D. Levy, A. Gulik, A. Bluzat, J.L. Rigaud, Biochim. Biophys. Acta 1107 (1992) 283–298.
[35] M. Chiesi, S.W. Peterson, O. Acuto, Arch. Biochem. Biophys. 189 (1978) 132–136.
[36] L.G. Reddy, L.R. Jones, S.E. Cala, J.J. O'Brian, S.A. Tatulian, D.L. Stokes, J. Biol. Chem. 270 (1995) 9390–9397.
[37] J.P. Anderson, E. Shriver, T.S. Mahrous, J.V. Moller, Biochim. Biophys. Acta 728 (1983) 1–10.
[38] B.D. Shivanna, E.S. Rowe, Biochem. J. 325 (1997) 533–542.
[39] B. De Foresta, M. le Maize, S. Orlowski, P. Champeil, S. Lund, J.V. Moller, F. Michelangeli, A.G. Lee, Biochemistry 28 (1989) 2558–2567.
[40] R.J. Barry, F.J. Canada, R.R. Rando, J. Biol. Chem. 264 (1989) 9231–9238.

[41] J. Kessi, R. Ghosh, R. Bachofen, Photosynth. Res. 46 (1995) 353–362.
[42] C.R. Sanders, Biophys. J. 64 (1993) 171–181.
[43] B.J. Hare, J.H. Prestegard, D.M. Engelmann, Biophys. J. 69 (1995) 1891–1896.
[44] O. Vinogradova, F. Sönnichsen, C.R. Sanders, J. Biomol. NMR 4 (1998) 381–386.
[45] C.R. Sanders, J.P. Schwonek, Biochemistry 31 (1992) 8898–8905.
[46] C.R. Sanders, B.J. Hare, K.P. Howard, J.H. Prestegard, Prog. NMR Spectrosc. 26 (1994) 421–444.
[47] C.R. Sanders, G.C. Landis, Biochemistry 34 (1995) 4030–4040.
[48] J.L. Eisele, J.P. Rosenbusch, J. Mol. Biol. 206 (1989) 209–212.